

Sound production biomechanics in three-spined toadfish and potential functional consequences of swim bladder morphology in the *Batrachoididae*^{a)}

Sang Min Han,^{1,2,b)}  Bruce R. Land,¹ Andrew H. Bass,² and Aaron N. Rice^{3,c)} 

¹*School of Electrical and Computer Engineering, Cornell University, Ithaca, New York 14853, USA*

²*Department of Neurobiology and Behavior, Cornell University, Ithaca, New York 14853, USA*

³*K. Lisa Yang Center for Conservation Bioacoustics, Cornell Lab of Ornithology, Cornell University, Ithaca, New York 14850, USA*

ABSTRACT:

The relationship between sound complexity and the underlying morphology and physiology of the vocal organ anatomy is a fundamental component in the evolution of acoustic communication, particularly for fishes. Among vertebrates, the mammalian larynx and avian syrinx are the best-studied vocal organs, and their ability to produce complex vocalizations has been modeled. The range and complexity of the sounds in mammalian lineages have been attributed, in part, to the bilateral nature of the vocal anatomy. Similarly, we hypothesize that the bipartite swim bladder of some species of toadfish (family *Batrachoididae*) is responsible for complex nonlinear characters of the multiple call types that they can produce, supported by nerve transection experiments. Here, we develop a low-dimensional coupled-oscillator model of the mechanics underlying sound production by the two halves of the swim bladder of the three-spined toadfish, *Batrachomoeus trispinosus*. Our model was able to replicate the nonlinear structure of both courtship and agonistic sounds. The results provide essential support for the hypothesis that fishes and tetrapods have converged in an evolutionary innovation for complex acoustic signaling, namely, a relatively simple bipartite mechanism dependent on sonic muscles contracting around a gas filled structure.

© 2023 Acoustical Society of America. <https://doi.org/10.1121/10.0022386>

(Received 29 June 2023; revised 25 October 2023; accepted 30 October 2023; published online 29 November 2023)

[Editor: Michael L. Fine]

Pages: 3466–3478

I. INTRODUCTION

The relationship between form and function in vocal systems is a thematic question in acoustic communication across vertebrates (e.g., Bradbury and Vehrencamp, 2011; Elemans *et al.*, 2015; Suthers *et al.*, 2016). In evaluating the diversity of animal sonation, an immediate question that emerges is what constitutes “acoustic complexity” in biological systems. Traditionally, acoustic complexity has been defined in a variety of different contexts, such as repertoire size (e.g., Grunst and Grunst, 2014), the number of notes in a song (Kroodsmma, 1980), or frequency modulation (Suthers *et al.*, 2016). In recent years, diverse taxa have been shown or suggested to contain a variety of nonlinear acoustic features in their calls (e.g., Fee *et al.*, 1998; Wilden *et al.*, 1998; Fitch *et al.*, 2002; Tokuda *et al.*, 2002; Beckers and ten Cate, 2006; Suthers *et al.*, 2006; Benko and Perc, 2009; Rice *et al.*, 2011), and this variety represents an additional axis of acoustic complexity to more traditional measures.

The different evolutionary histories across vertebrates have given rise to a wide diversity of mechanical

mechanisms for producing sounds (e.g., Suthers *et al.*, 2016; Ladich and Winkler, 2017). In most tetrapods, a common mechanism of the larynx and syrinx is the coupling of vocal fold oscillation with air movement (Goller and Riede, 2013; Elemans *et al.*, 2015). In fishes, one of the common sonic mechanisms is swim bladder vibration (Rice *et al.*, 2022), and (Fine and Parmentier, 2022), the acoustic properties of emitted sounds depend on this gas filled organ and its associated muscles (e.g., Skoglund, 1961; Fine, 1983; Barimo and Fine, 1998; Fine *et al.*, 2001; Fine *et al.*, 2002; Fine and Parmentier, 2022).

A number of characters, including evolutionarily conserved central mechanisms responsible for sound production in fishes and tetrapods (Bass and Chagnaud, 2012), render the term “vocalization” appropriate for describing sounds produced by fishes (Bass *et al.*, 2015; Bass and Rice, 2010). Recent work in toadfishes (e.g., Amorim *et al.*, 2008; Rice *et al.*, 2011; Elemans *et al.*, 2014) shows that fishes can achieve a level of vocal complexity that sometimes includes nonlinear features such as deterministic chaos, frequency jumps, and subharmonics (see reviews by Wilden *et al.*, 1998; Fitch *et al.*, 2002). In the three-spined toadfish, *Batrachomoeus trispinosus*, nonlinear sounds are produced by a longitudinally divided swim bladder with each half having one sonic muscle attached to its outer wall (Fig. 1) (Rice and Bass, 2009; Rice *et al.*, 2011). The bilateral nature of the

^{a)}This paper is part of a special issue on Fish Bioacoustics: Hearing and Sound Communication.

^{b)}Present address: Department of Electrical Engineering and Computer Sciences, University of California, Berkeley, CA 94720, USA.

^{c)}Email: arice@cornell.edu

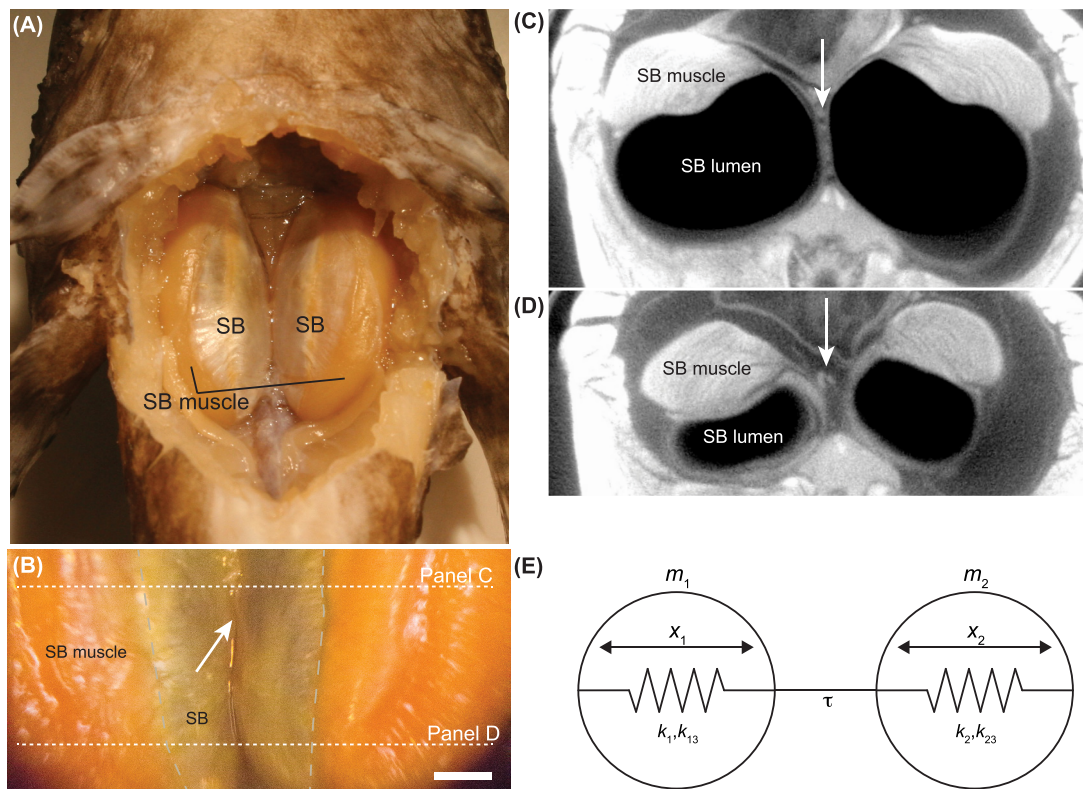


FIG. 1. (Color online) Anatomy of the *Batrachomoeus trispinosus* swim bladder. (A) Ventral view of the swim bladders *in situ*, showing the swim bladder (SB), and swim bladder muscle (SB muscle). Muscle fibers in the swim bladder are oriented and contract radially. (B) Enlarged *in situ* ventral view of the posterior end of *B. trispinosus* swimbladder, showing the swim bladder (SB), swim bladder muscle (SB muscle), and collagenous connective tissue between the bladders (white arrow). The gray vertical dashed line indicates the medial division between the swim bladder muscle and the swim bladder wall. The white horizontal dashed lines indicate the approximate “slice” position of μ CT images in (C) and (D). The scale bar (lower right) represents 2 mm. Note: the bladders in (A) and (B) are from different individuals. (C), (D): Transverse view of μ CT image of toadfish midsection ($25\ \mu\text{m}$ slice thickness), showing the swim bladder muscle, swim bladder lumen (SB lumen), and connective tissue (white arrow). The bladders are in contact with dense soft tissue along the dorsal body wall but do not make direct contact with the vertebral column. This specimen was stained with KI to enhance soft tissue resolution (Gignac and Kley, 2014). (E) Simplified low-dimensional mechanical model of the *B. trispinosus* swim bladder.

swim bladder in *B. trispinosus* and other close relatives (see Rice and Bass, 2009) is reminiscent of the lateralized tissue oscillations in the songbird syrinx (though lacking independent neuromuscular control) or mammalian larynx (Riede and Goller, 2010b). However, the swim bladder mechanics underlying *B. trispinosus* vocal complexity is a simpler case than the syrinx because it does not depend on air movement for sound production.

An additional advantage of using toadfishes as a model for understanding the neuromechanics of vocalizations is the opportunity to distinguish the role of central and peripheral mechanisms in sound production. A single pattern generator network in the caudal hindbrain comprised of three separate neuronal populations establishes the final activity pattern of the sonic muscles and, in turn, the duration, pulse repetition rate (also sets the fundamental frequency for multi-harmonic signals), and amplitude modulation pattern of natural calls (Chagnaud *et al.*, 2011). While this network clearly establishes these temporal properties, complex acoustic features such as nonlinearities would depend on the biomechanical performance of peripheral organs such as the swim bladder (Bass and Ladich, 2008; Rice *et al.*, 2011); however, there is evidence suggesting that some

signals with nonlinear features originate in motor patterns and are not results of swim bladder or muscles (Elemans *et al.*, 2014).

There has been over a century of bioacoustics work on toadfish sounds (e.g., Gudger, 1908; Tower, 1908), and the species *Halobatrachus didactylus*, *Opsanus beta*, *Opsanus tau*, and *Porichthys notatus* remain among the best studied among sonic fishes (e.g., Amorim *et al.*, 2008; Bass, *et al.*, 2015). Toadfishes comprise a single order and family (Batrachoidiformes, Batrachoididae) with about 25 genera and 78 species (Greenfield *et al.*, 2008). Of the currently described 84 species within the Batrachoididae (Fricke *et al.*, 2023), only a small number of species have had their sounds described or recorded (summarized in Rice and Bass, 2010; Mosharo and Lobel, 2012); only a small proportion have had their swim bladder morphology described, revealing variation across the family (Tower, 1908; Fänge and Wittenberg, 1958; Lane, 1967; Lancey, 1975; dos Santos *et al.*, 2000; Rice and Bass, 2010; Chiu *et al.*, 2013; Vaz, 2020). The role of swim bladder morphology in toadfish acoustic signal generation has only been well-studied in *Opsanus tau* and *Porichthys notatus* (Fine *et al.*, 2001; Fine *et al.*, 2002; Rice and Bass, 2010; Rice *et al.*, 2011; Fine *et al.*, 2016). Examining evolutionary

patterns of different swim bladder shapes within toadfishes can help contextualize biomechanical mechanisms that are being used for sound production and responsible for signal diversity.

Focusing on the unique *B. trispinosus* swim bladder morphology, we explore how this relatively simple vocal motor system can produce both simple and complex vocalizations with bilaterally separated swim bladder halves. We developed a low-dimensional coupled-oscillator model of the *B. trispinosus* swim bladder dynamics to explain how simple and complex sounds are generated. Similar to work on the avian syrinx (Fee *et al.*, 1998; Larsen and Goller, 1999; Zollinger *et al.*, 2008), our coupled-oscillator model of toadfish sounds demonstrates how the interaction of lateral vocal mechanisms gives rise to a diversity of sounds.

II. MATERIALS AND METHODS

A. *Batrachomoeus trispinosus* sounds and specimens

Similar to other toadfishes, *B. trispinosus* use their swim bladder to produce several different call types (Rice

and Bass, 2009), but here we focus on two that diverge widely in their spectral and temporal properties: “hoots” and “grunts” [Figs. 2(A) and 2(C)]. Hoots are advertisement calls likely used in reproductive contexts (Rice and Bass, 2009), are harmonic in their spectral structure, and last approximately 0.5–1.75 s [Fig. 2(A), Mm. 1]. Grunts are agonistic calls (Rice and Bass, 2009), broadband, and last 0.25–0.5 s [Fig. 2(C), Mm. 2]. Both call types are regularly produced in successive calling bouts and sometimes exhibit different nonlinear characteristics such as deterministic chaos and biphonation (Rice and Bass, 2009; Rice *et al.*, 2011). Sounds used in analyses here were recorded from a captive population of freely behaving individuals in community tanks (see Rice and Bass, 2009). Grunts were produced by both males and females, but hoots were produced by only males (Rice and Bass, 2009).

Mm. 1. A recording of representative hoot from freely moving *Batrachomoeus trispinosus* recorded in aquaria with conspecifics.

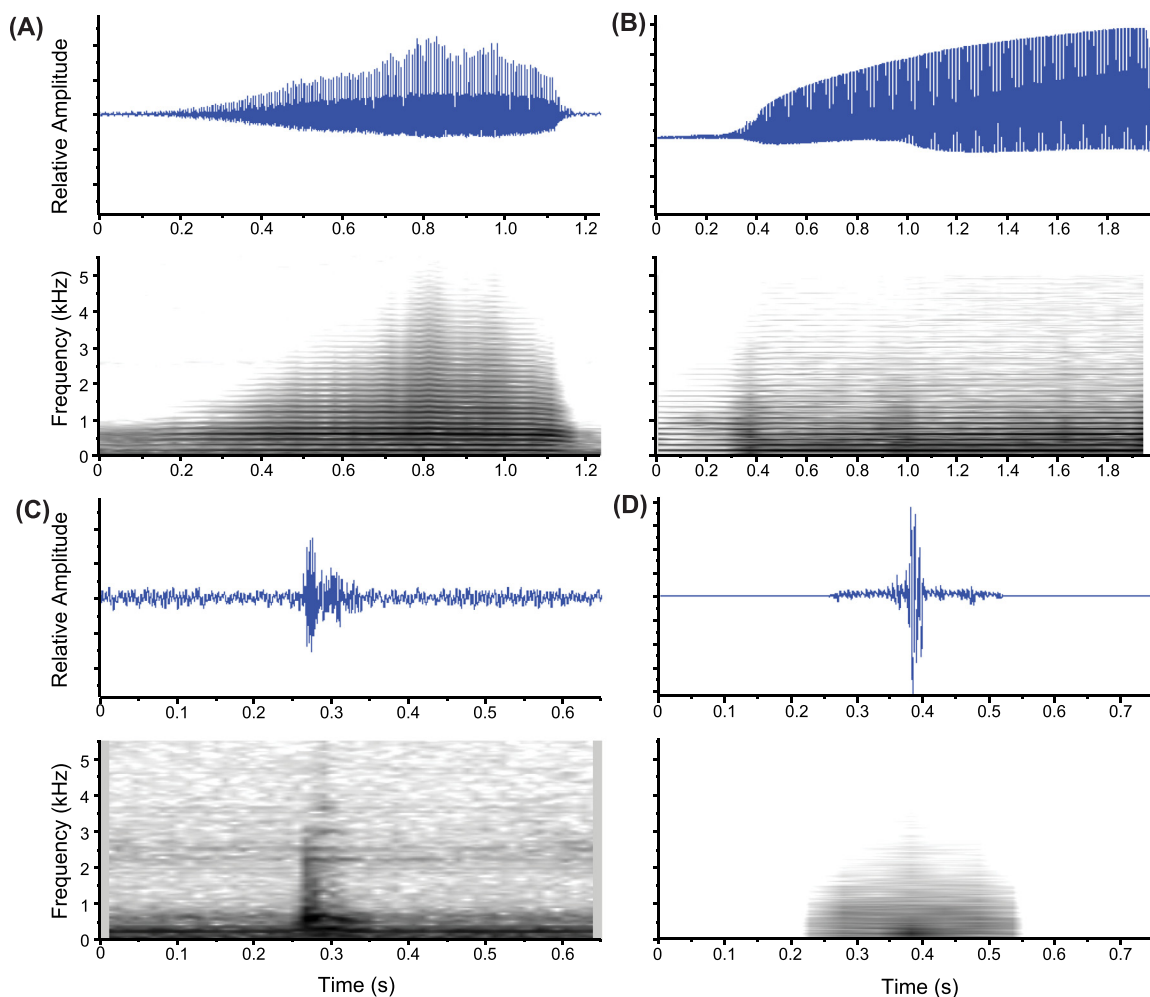


FIG. 2. (Color online) Representative calls recorded from *Batrachomoeus trispinosus*. (A) Waveform (top) and spectrogram (bottom) of hoot recorded from freely moving captive fish in aquaria. (B) Waveform (top) and spectrogram (bottom) of modeled hoot (see the text for modeling parameters). (C) Waveform (top) and spectrogram (bottom) of grunt recorded from freely moving captive fish in aquaria. (D) Waveform (top) and spectrogram (bottom) of modeled grunt. Insets in panels (A) and (C) show waveform scaled with relative amplitude on the y-axis. Sounds in (A) and (C) are from Rice *et al.* (2011). Spectrograms were generated in Raven Pro 1.65, fast Fourier transform (FFT) = 1024 pt, 75% overlap.

Mm. 2. A recording of representative grunt from freely-moving *Batrachomoeus trispinosus* recorded in aquaria with conspecifics.

Batrachomoeus trispinosus specimens for morphological analysis were obtained through the aquarium trade (Pet Solutions, Beavercreek, OH) and preserved in formalin. Specimens for μ CT imaging were stained with potassium iodide to enhance soft-tissue contrast (Gignac and Kley, 2014). Fish were scanned with a high-resolution μ CT (GE eXplore CT-120, GE Healthcare, London, Ontario, Canada) at 25 μ m thickness. Images were reviewed using the Horos DICOM viewer (horosproject.org).

B. Vocal system biomechanical model

Observations through a dissecting microscope [Figs. 1(A) and 1(B)] together with high-resolution μ CT scanning [Figs. 1(C) and 1(D)] revealed that the two swim bladder halves (and their lumens) are physically separate but enmeshed in fascia and other collagenous, tendon-like, connective tissue. In freshly dissected specimens, the swim bladder walls appeared rigid, suggesting a high internal pressure. From a mechanical perspective, while vibration forces are bilaterally and independently generated by each swim bladder muscle, these soft tissue interconnections might transmit forces between the two bladder halves. By representing this anatomy and linkages as a one-dimensional system, it allows us to model the paired bladders as a simple mechanical system of two coupled oscillating spring masses (Fig. 1E). The dynamics of this system are represented by Eqs. (1) and (2). Each equation describes the physics of one oscillator that models each side, i.e., one swim bladder,

$$\frac{d^2x_1}{dt^2} = -k_1x_1 - k_{13}(x_1 - x_0)^3 - d_1 \frac{dx_1}{dt} - f + \tau \frac{(x_1 - x_2)^7}{1 + (x_1 - x_2)^7}, \tag{1}$$

$$\frac{d^2x_2}{dt^2} = -k_2x_2 - k_{23}(x_2 - x_0)^3 - d_2 \frac{dx_2}{dt} + f - \tau \frac{(x_1 - x_2)^7}{1 + (x_1 - x_2)^7}, \tag{2}$$

where x_0 is the reference position, x_1 and x_2 are absolute positions, k_1 and k_2 are linear spring constants, k_{13} and k_{23} are nonlinear cubic spring constants, d_1 and d_2 are linear velocity-dependent damping terms of the first and second oscillators, respectively, f is the motor output from the central nervous system driving muscle activation, and τ is the magnitude of the force exerted by the tendon connecting the two swim bladders. Figure 1(E) is a diagram of this dynamical system.

Like other toadfishes (Bass and Baker, 1991; Chagnaud and Bass, 2014), neurophysiological experiments on batrachoidid fishes show that swim bladder muscles are driven simultaneously by the hindbrain network output Chagnaud

and Bass, 2014). This muscle force, denoted by f in Eqs. (1) and (2), is a sawtooth wave function that contracts and relaxes the muscles driving the swim bladder, which is modeled on muscle tension measurements (McMahon, 1984). This sawtooth wave function is ramped up to a set of muscle amplitudes, one for each oscillator, before ramping back down. The linear envelopes prevent transient artifacts caused by the sudden onset of input energies and provide a simple mechanism for recreating the gradual changes in sound amplitude observed over the course of a call. These two envelopes of sawtooth wave functions make up the driving forces for the two oscillators. We used a swim bladder muscle contraction rate of 150 Hz, which corresponds to the approximate fundamental frequency of the *B. trispinosus* call at 26 °C (Rice and Bass, 2009). While the fundamental frequency of toadfish calls varies with temperature (e.g., Fine, 1978; Brantley and Bass, 1994; Fournet *et al.*, 2022), we did not vary temperatures in the model due to the lack of information on *B. trispinosus* temperature preferences. (Greenfield, 2001).

The two swim bladders oscillate inside the abdominal cavity, leading the body walls to move water, which physically acts like a mass. The system together acts like oscillating spring masses, one for each bladder. The resonant vibrational frequency of a spring oscillator is given by the equation

$$\text{freq} = \frac{1}{2\pi} \sqrt{\frac{k}{m}}, \tag{3}$$

where k is the spring constant and m is the mass of the oscillator. Because the mass of each swim bladder is fixed and scaled to 1 in the model, the time scale and natural frequency of the system are largely determined by the spring constants. The resistive forces caused by the viscous drag of internal body fluids and friction resulting from the swim bladders contacting the body walls are accounted for by the damping terms.

The model includes nonlinear cubic spring constants, which represent the compressibility of air inside each swim bladder. These nonlinear factors, however, are insignificant as our results show, and thus can be omitted from the model. The cubic spring constant term was fixed at 0.1 for air compressibility. The tissue connecting the two swim bladders may be important for generating complex nonlinear features in *B. trispinosus* vocalizations. The connecting tissue is towards the posterior end of the swim bladders, and as the bladders contract radially, we hypothesize that the posterior ends of the bladder move outwards, stretching the length of the connecting tissue. The tissue is similar to a string that becomes stiff and exerts force when stretched by the oscillators; because the tissue shows no sign of a lumen or muscle fibers, we assume it may be a tendon, or share similar properties (e.g., Alexander, 2002; Summers and Koob, 2002). The force acted on by the tissue is modeled by the term with coefficient τ that depends on the distance between the two oscillators, the length of the tendon, raised to the seventh

power (Fouré *et al.*, 2013). The seventh power was determined by empirically fitting a polynomial curve to the observed relationship between tendon force and tendon elongation length [see Fig. 16(A) in Fouré *et al.*, 2013]. Tendons vary in their force transmission based on their structure (Alexander, 2002; Summers and Koob, 2002), so the empirical values used for modeling here are presumptive. Sensitivity analyses on the tendon length exponent showed that the model is robust to slight variations in the exponent of the power term. The model yielded very similar results when using different exponent values (3, 5, and 7). These exponent values were chosen such that the curves describing the tendon force term and the aforementioned fitted polynomial exhibited the same end behaviors. All model parameters are normalized to the length of the tendon.

With the tendon force coefficient fixed, we determined that three pairs of model parameters: spring constants, damping terms, and muscle amplitudes, one for each swim bladder, comprehensively determine the characteristics of a simulated toadfish call. The ratio of the two spring constants reflects the relative size difference of one swim bladder to another, and this varies across individuals (Rice and Bass, 2009). The ratio of the two swim bladders in toadfish was measured to be approximately 0.5; the lateral radius of one swim bladder is approximately twice as large as its counterpart in a typical toadfish (Rice and Bass, 2009). Therefore, the ratio of the two spring constants is fixed to 0.5 in the model. Due to the similar environment in which the swim bladders oscillate, and the symmetric muscle drives in toadfish, the ratios of damping terms and muscle amplitudes are fixed to 1. These fixed ratios reduce the dimensionality of the model to three dimensions, considerably simplifying the complexity of the model.

1. Numerical solution

Equations (1) and (2) convert the biomechanical model into a system of two coupled second-order ordinary differential equations. Because a strong nonlinearity exists in the dynamics of the system: the tendon only acts a negligible amount of force on the system until it is pulled tighter, the system can be characterized as “stiff.” We therefore use the stiff numerical ordinary differential equations solver *ode15s* in MATLAB to find the solutions of the *B. trispinosus* swim bladder system described by Eqs. (1) and (2). The solutions of this system are the positions and velocities of the two swim bladders. The difference between the two bias-corrected (mean-adjusted) swim bladder positions yielded a simulated toadfish call waveform [Fig. 2(B); Mm. 2].

2. Optimization

Via mathematical optimization, we find the set of model parameters producing simulated sounds that best match naturally evoked *B. trispinosus* calls. With the ratios of the three comprehensive sets of model parameters fixed as invariants after taking into account known physical properties of the swim bladder as described previously, the three

model parameters: spring constant, damping term, and muscle amplitude, are taken as the decision variables of the optimization problem. Specifically, we use the MATLAB function *fminsearch* that employs the Nelder-Mead simplex direct search algorithm (Olsson and Nelson, 1975) to perform a heuristic search for the set of model parameters that yields a simulated toadfish call of best fit given an empirical recording of an actual toadfish call. With this algorithm, we solve the following unconstrained nonlinear optimization problem:

$$\min_q \frac{1}{N} \sum_f (S(f) - \hat{S}(f))^2, \quad (4)$$

where $S(f)$ is the magnitude of the power density spectrum of the empirical toadfish call recording and $\hat{S}(f)$ is the magnitude of the power density spectrum of the simulated toadfish call at frequency f , $q \in \mathbb{R}^3$ is a vector with the spring constant, damping term, and muscle amplitude as its elements in the stated order, and N is the number of frequency bins.

In order to determine the optimal set of model parameter values q^* required to best simulate the toadfish call of interest, we compare the power density spectra of the system solutions at different sets of model parameter values q encountered along the heuristic search to the power density spectrum of the empirical toadfish call recording, which serves as the basis for quantitative comparison for the simulated sounds (Fig. 2). As described by the optimization problem, the heuristic optimizer minimizes the mean squared error between the power density spectra of the model generated and recorded sounds. We compared the spectral energies of the empirical and simulated sounds at every frequency. In an effort to further decrease the differences between the calculated and observed power density spectra, we adjusted the two spectra so that they are biased at the same level by subtracting the absolute difference of the means of the two spectra from the spectrum with a higher mean.

The optimization problem is not convex with respect to the decision variables. The Nelder-Mead simplex direct search algorithm therefore is limited in efficacy because the algorithm cannot discern the objective function’s local minimum from its global minimum. The optimizer converges only to local minima. Because the ratios of each parameter pair are fixed for low-dimensionality and parameters for only one swim bladder oscillator are used as model inputs, the optimization problem’s cost function can be visualized using three-dimensional isosurfaces. Isosurfaces are surfaces of constant objective function value, with each dimension representing one of the three model parameters. These isosurfaces collectively comprise the three-dimensional scalar field representation of the function specified by Eq. (4), where points in each colored surface represent sets of the three model parameter values that yield a constant evaluated function value. These isosurfaces graphically point out the approximate location of a potential global minimum, and

the set of model parameters in the proximity of the isosurface corresponding to the lowest cost function value is used as the initial guess for the heuristic search algorithm.

The algorithm also introduces another obstacle in solving the minimization problem. The optimizer often flounders in a neighborhood of a local minimum and fails to converge before exhausting its set number of maximum iterations. As a workaround to this issue, we randomly perturb the optimization variable after a set number of iterations until convergence, which is inspired by ideas in stochastic optimization algorithms such as simulated annealing.

C. Morphological diversity of toadfish swim bladders

To place the functional model of *B. trispinosus* sound generation in the context of the wider morphological diversity of toadfish swim bladders, museum specimens representing different toadfish genera were obtained (see supplementary material). Gross swim bladder morphology for *Halobatrachus didactylus* was taken from dos Santos *et al.* (2000); *Aphos porosus*, *Batrachthys apiatus*, and *Riekertia ellisi* are from Vaz (2020). Because many toadfish species are limited to type specimens in most museum collections, we were limited to species with multiple specimens in lots that were suitable for limited dissection and visual inspection of the swim bladder. Due to the age of the examined specimens and the intrusion of liquid into the swim bladder lumen, most of the museum specimens were not suitable for computed tomography (CT) analysis. A small ventral incision in the specimens was used to expose the swim bladder, where swim bladder morphology was documented under a dissecting microscope and measured with

calipers. The outlines of the gross morphology of each species' examined swim bladder were mapped onto a phylogenetic tree of the Batrachoididae (see Figs. 77 and 80 from Greenfield *et al.*, 2008).

III. RESULTS

A. *Batrachomoeus trispinosus* hoots

In the recording of a representative *B. trispinosus* "hoot" analyzed here, call amplitude increased for approximately the first two-thirds of the call (1.37 s), and then decreased for the duration of the call (0.28 s) [Fig. 2(A)]. To best simulate this call characteristic, the envelope of the muscle drive (a periodic sawtooth wave) was increased linearly to the muscle amplitude of the decision variable in 1.95 s and then rapidly decreased linearly for the remaining 0.05 s. Before optimizing the model parameters, we calculated the mean squared errors of the simulated sounds at various decision variable values using the empirical toadfish hoot to generate three-dimensional isosurfaces. We selected ranges of model input parameters large enough to yield an enclosed isosurface. Figure 3 shows the set of isosurfaces used to locate the initial guess for the heuristic optimization algorithm.

Surfaces corresponding to increasing mean squared error (cost function) values are depicted in colors of increasing frequencies or decreasing wavelengths, i.e., the red isosurface represents the collection of model parameter values that yield a lower error value than that represented by the sets of model parameter values comprising the blue isosurface. The red isosurface is the isosurface of best fit, which

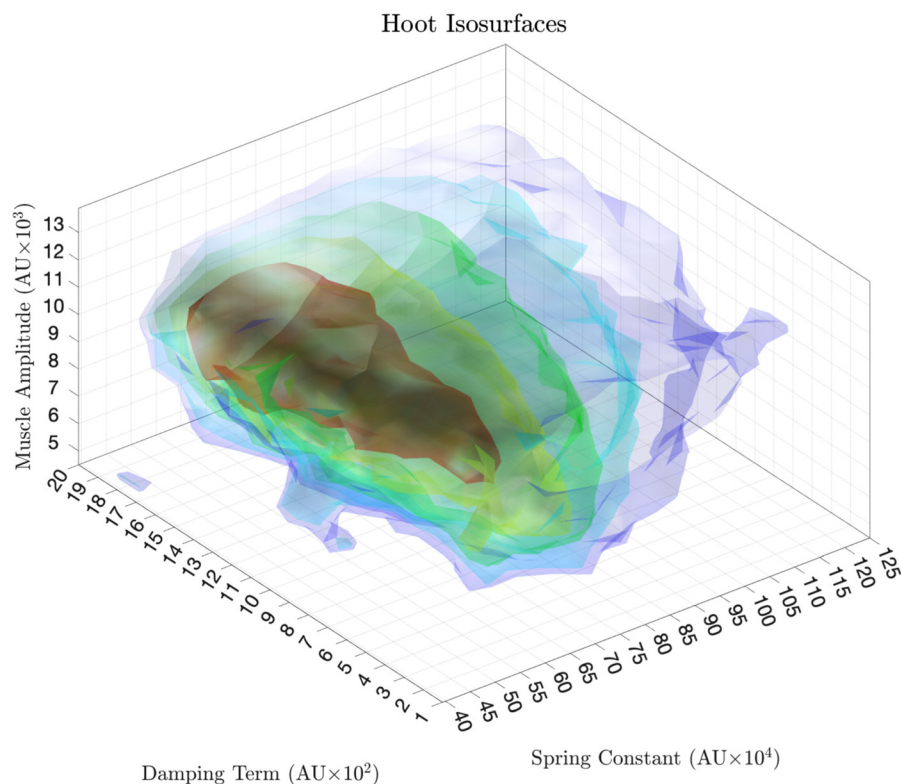


FIG. 3. (Color online) Isosurfaces of constant mean squared error values showing the differences between the spectra of an empirical toadfish hoot and computer-generated simulated hoots for sets of spring constant, damping term, and muscle amplitude values. Isosurfaces corresponding to increasing mean squared error (cost function) values are depicted in colors of increasing frequencies or decreasing wavelengths, and an enclosed best-fit isosurface is shown colored in red.

corresponds to the visible isosurface pertaining to the smallest objective function—mean squared error—value. We concluded from this isosurface that the global minimizer, if it exists, must reside somewhere inside this enclosed isosurface of best fit.

After obtaining an enclosed best-fit isosurface, we solved for the optimal toadfish hoot waveform by solving the coupled-oscillator system at the optimized set of model parameters: the spring constant, damping term, and muscle amplitude, which we obtained by running the aforementioned Nelder-Mead simplex direct search algorithm initialized at a set of model parameters slightly perturbed from the center of the best-fit isosurface in Fig. 3. As expected, the heuristic optimizer converged to an optimal point in the three-dimensional space within the enclosed best-fit isosurface. The solutions of the system described by Eqs. (1) and (2) are the oscillation waveforms of the two modeled swim bladder masses. The mean-adjusted difference of these two individual waveforms obtained using the optimal set of model parameters is the waveform of the simulated sound [Fig. 4(A), Mm. 3]. The power density spectrum of the synthetic call [Fig. 4(B)] closely resembles that of the natural call [Fig. 4(C)]. The spectrogram of the simulated sound contains features of nonlinearity such as the presence of sub-harmonic features as well as the sudden onset and offset of bursting energies [Fig. 4(D)].

Mm. 3. Sound file of simulated hoot of *Batrachomoeus trispinosus* generated with coupled-oscillator model.

B. *Batrachomoeus trispinosus* grunts

The same biomechanical model [Fig. 1(E)] was used to simulate *B. trispinosus* grunts. In the recording of a typical toadfish grunt that we used, the toadfish releases a shorter duration sound that lasts for 0.3 s [Fig. 2(C)]. To best simulate this call characteristic, the envelope of the muscle drive, a periodic sawtooth wave, was increased linearly to the muscle amplitude of the decision variable in 0.15 s and then decreased linearly to silence in 0.15 s. We again solved the system at various sets of model parameters to obtain the set of isosurfaces for grunts (Fig. 5, Mm. 4). Enclosed isosurfaces interestingly could not be obtained using a biophysically reasonable range of model parameters for a grunt, but this did not hinder the algorithm’s ability to converge to an optimum.

Mm. 4. Sound file of simulated grunt of *Batrachomoeus trispinosus* generated with coupled-oscillator model.

We used the set of model parameters located inside the largest region of the best-fit isosurface (red) as the initialization point for the heuristic optimizer. Despite the absence of an enclosed best-fit isosurface, the optimizer converged to a set of model parameters within the best-fit isosurface. Results for the optimal simulated toadfish grunt are shown in Fig. 6. We see that the model generated sound contains features closely resembling those of natural toadfish vocalization. The mean-adjusted difference waveform [Fig. 6(A)] shows a short duration call with a peak amplitude

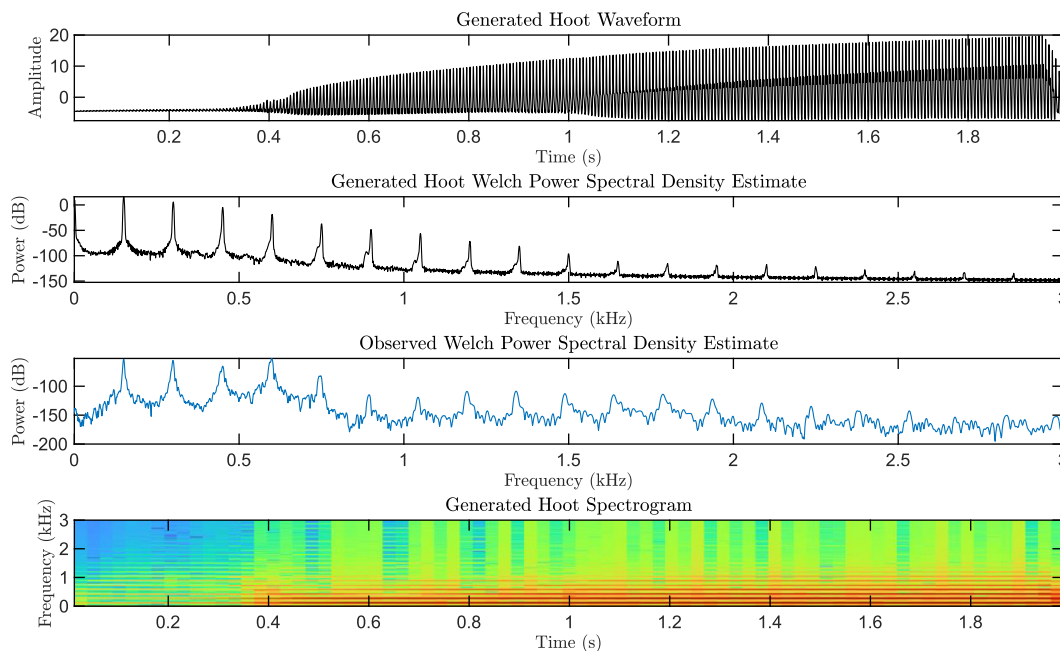


FIG. 4. (Color online) Spectral features of *Batrachomoeus trispinosus* synthetic and natural hoots. A synthetic hoot was generated with the optimized set of parameters near the center of the best-fit isosurface, where $k_1 = 4.2435 \times 10^5$, $k_2 = 8.4869 \times 10^5$, $d_1 = 998.8594$, $d_2 = 998.8594$, $amp_1 = 8.0559 \times 10^3$, and $amp_2 = 8.0559 \times 10^3$. (A) Bias-corrected difference of the waveforms of the two swim bladder oscillators; this waveform yields the synthetic hoot. (B) Calculated power density spectrum of the optimal computer-generated toadfish hoot. (C) Observed power density spectrum obtained from a recording of a natural toadfish hoot. (D) Spectrogram of the optimal computer-generated toadfish hoot.

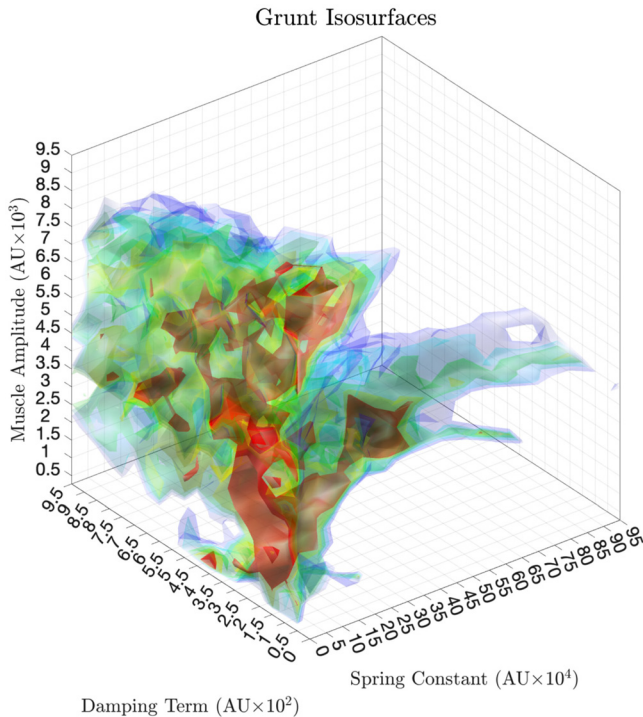


FIG. 5. (Color online) Isosurfaces of constant mean squared error values showing the differences between the spectra of an empirical toadfish grunt and computer-generated simulated grunts for sets of spring constant, damping term, and muscle amplitude values. Isosurfaces corresponding to increasing mean squared error values are depicted in colors of increasing frequencies or decreasing wavelengths, and the best-fit isosurface is shown colored in red.

approximately 0.15 s into the call. The power density spectrum of the simulated call [Fig. 6(B)] shows a clear harmonic structure at the fundamental frequency and first harmonic, more so than the naturally recorded grunt [Fig. 6(C)]. The spectrogram of the simulated sound shows spectral properties consistent with deterministic chaos, similar to what is observed in natural calls [Fig. 2(B)].

C. Morphological diversity of toadfish swim bladders

Ten additional toadfish species, representing eight genera were examined (see supplementary material, Table S1). Swim bladders exhibited a range of morphologies, from single cardioid shapes (e.g., *Opsanus*, *Porichthys*, *Daector*) to lateral halves of the swim bladder connected via a duct (e.g., *Halobatrachus*, *Allenbatrachus*), to the swim bladder halves being connected via a tendon (i.e., *Batrachomoeus*). When these morphologies are mapped onto a genus-level, strict consensus phylogenetic tree of toadfishes (see Figs. 77 and 80 in Greenfield *et al.*, 2008), the single cardioid swim bladder maps are found in “New World” toadfishes (those genera found in the Western Hemisphere), while the separated swim bladders are found in “Old World” toadfishes (those genera found in the Eastern Hemisphere) (Fig. 7).

IV. DISCUSSION

We found that a one-dimensional coupled-oscillator model can produce two widely divergent call types from the three-spined toadfish *B. trispinosus*. Thus, despite the

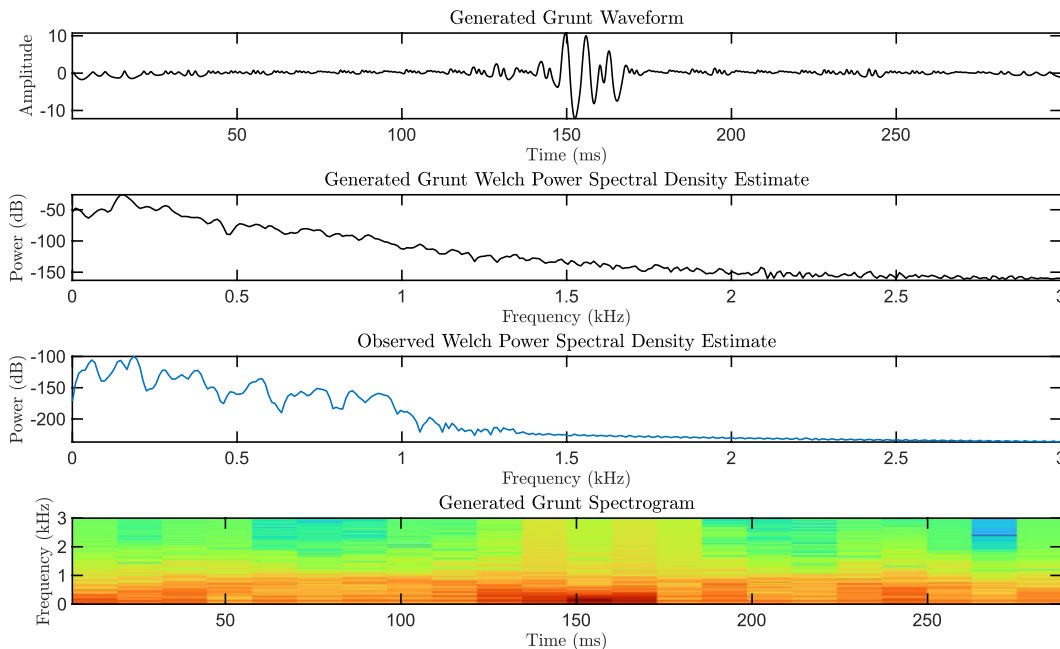


FIG. 6. (Color online) Spectral features of *Batrachomoeus trispinosus* synthetic and natural grunts. A synthetic grunt was generated with the optimized set of parameters within the best-fit isosurface, where $k_1 = 7.7915 \times 10^4$, $k_2 = 1.5583 \times 10^5$, $d_1 = 150.7949$, $d_2 = 150.7949$, $amp_1 = 3.1799 \times 10^3$, and $amp_2 = 3.1799 \times 10^3$. (A) Bias-corrected difference of the waveforms of the two swim bladder oscillators; this waveform yields the synthetic grunt. (B) Calculated power density spectrum of the optimal computer-generated toadfish grunt. (C) Observed power density spectrum obtained from a recording of a natural toadfish grunt. (D) Spectrogram of the optimal computer-generated toadfish grunt.

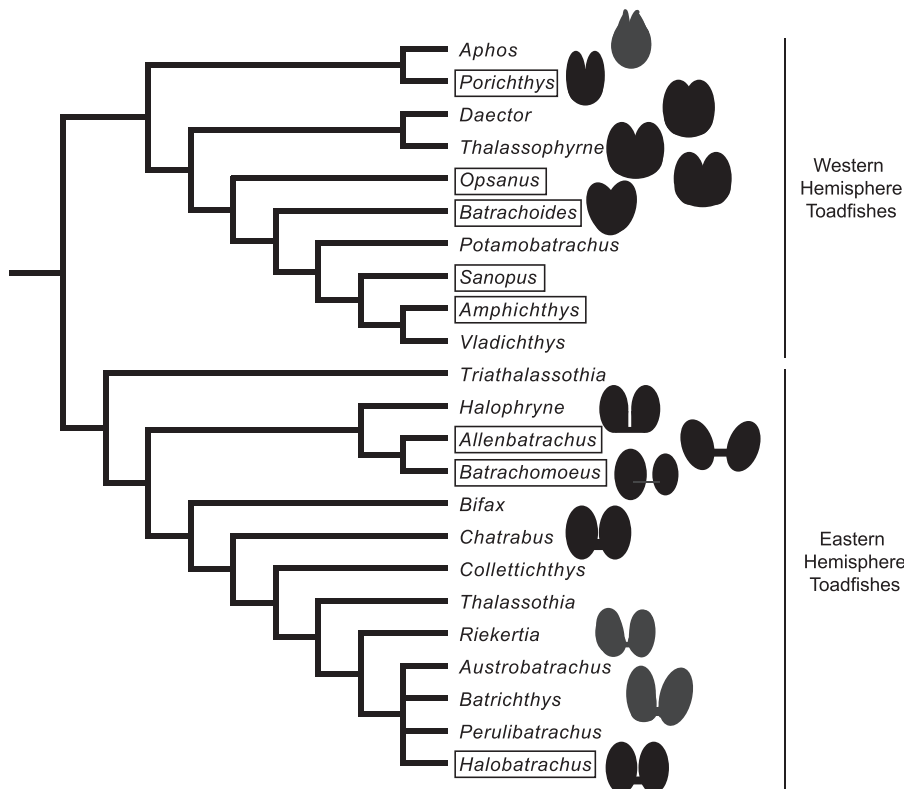


FIG. 7. Evolutionary diversity of toadfish swim bladders. Swim bladder outlines are mapped onto data from the strict consensus phylogenetic tree of Greenfield *et al.* (2008) showing valid genera within the Batrachoididae. Names of genera in a box are those taxa that have had sounds recorded or described (dos Santos *et al.*, 2000; Mosharo and Lobel, 2012; Chiu *et al.*, 2013; Staaterman *et al.*, 2018).

complex acoustic structure of the sounds (Rice and Bass, 2009; Rice *et al.*, 2011), the biomechanics of sound generation are comparatively simple and largely influenced by the interaction of the three physiologically-relevant variables—muscle amplitude, swim bladder damping, and bladder resonance—included in our model. The low-dimensional aspect of the model and the resulting close correspondence between the modeled and natural sounds suggest that these variables play a critical role in sound generation *in vivo* (following Alexander, 2003).

Both the modeled hoot and grunt closely resembled sounds from live *B. trispinosus* recorded in captivity (Fig. 2). The pattern of amplitude modulation in the waveform and fundamental frequency were set as assumptions in the model, but both modeled sounds showed the spectral structure and nonlinear features seen in the recorded sounds. As vocal central pattern generator (CPG) activity and, in turn, sonic muscle contraction speed set the pulse repetition rate/fundamental frequency of toadfish calls (e.g., Bass and Baker, 1990), it is possible that the two other physiological inputs of the model, resonance and damping, may be responsible for producing nonlinearities and harmonic structure. It is intriguing that in the optimized isospace predictions of the hoot and grunt, the local optima are in different locations of isospace: optimal grunts are produced with lower muscle amplitudes and spring constants than hoots (Figs. 3 and 5). The optimization and isospace results suggest that hoots and grunts have different physiological mechanisms to produce them.

One intriguing observation in the naturally-evoked and synthetic hoot [Figs. 2(A) and 2(B)] is the asymmetry in the

waveform that is present in some but not all natural calls. The synthetic hoot waveform is the result of taking the mean-adjusted difference between the two swim bladder oscillator positions. Since one swim bladder has a rest position of 1 and another at 1.9, the difference sound waveform is not centered at 0 near the beginning when the muscle drive has not yet increased up amplitude. Because of the swim bladder oscillators' size difference, and thus the spring constant value difference, one oscillator position waveform dominates the other (one oscillator has a higher mean as well), causing asymmetry in the difference sound waveform. This may be how sound is produced in *B. trispinosus*, but recording via hydrophone or another device underwater outside the body cavity minimizes this asymmetry, though asymmetry in the waveform is present in some recordings of hoots [Fig. 2(A)]. We observed fewer asymmetries in grunts likely because the muscle drives are weaker and the sound durations are significantly shorter.

The variation in sounds and swim bladder structures across the toadfishes point to the dynamic and complex nature of the peripheral vocal system (Rice and Bass, 2009). However, the exact nature of how the mechanics of the swim bladder itself contribute to the generation of sounds remains unclear (Fine *et al.*, 2001; Fine *et al.*, 2016). It is also unclear whether there are corresponding differences in material properties across toadfish swim bladders in addition to variation in gross morphology that may contribute to variation in vocal features (Fine *et al.*, 2016). The *Opsanus* swim bladder is a highly damped structure, so it likely does not serve as a resonator (Fine, 1983; Fine *et al.*, 2001; Fine *et al.*, 2016), raising questions about the bladder's involvement in *Opsanus* sound

production (Fine *et al.*, 2001; Fine *et al.*, 2016). However, modeling and physical measurements of the plainfin midshipman, *Porichthys notatus*, swim bladder reveals that it has resonant modes at 110 Hz (near the fundamental frequency) and 350 Hz (Lancey, 1975), all within the fish's hearing range (McKibben and Bass, 1999; Sisneros and Bass, 2003; Sisneros and Bass, 2005). One of the more compelling pieces of evidence for an active role of the swim bladder in sound production comes from *P. notatus* males that actively inflate their swim bladder during prolonged courtship vocalizations (Bass *et al.*, 2015), and this may contribute to resonance or harmonic properties. To further add to the complexity of this bladder and muscle system, there are likely several competing demands on swim bladder function: the anterior horns of the *P. notatus* swim bladder may make the sound field non-omnidirectional to minimize interference with the fish's auditory receptive field (Forbes *et al.*, 2006; Mohr *et al.*, 2017). However, there is also empirical evidence against the importance of resonance in swim bladders (Fine and Parmentier, 2022), as the bladder in some species and conditions is a highly damped structure and thus would not be a resonant structure (Fine *et al.*, 2016; Sprague *et al.*, 2022). More examination of the material properties of *B. trispinosus* swim bladders would help clarify whether the structure exhibits more of a forced or resonant response (Fine and Parmentier, 2022).

Toadfish evolutionary relationships have been primarily established through either genetics or osteological morphological characters (Greenfield *et al.*, 2008; Vaz and Hilton, 2020), yet the correspondence between swim bladder gross morphology and phylogenetic relationships among toadfish genera raises intriguing form-function questions about the evolution of acoustic communication and the underlying peripheral mechanisms. All genera in the eastern hemisphere clade show bilaterally separated swim bladder halves connected by either a duct or connective tissue or tendon, and we predict that our coupled-oscillator model developed here for *B. trispinosus* may be appropriate for modeling sound generation mechanics in these taxa. Additionally, the morphological diversity in eastern hemisphere toadfishes (Fig. 7) suggests a wider diversity of signal structure in this clade compared to western hemisphere toadfishes, although investigation of sounds and morphology from more species is needed to test this hypothesis. Last, the phylogenetic mapping of toadfish swim bladders suggests that the “tendon” we observed connecting the bilateral halves of the *B. trispinosus* swim bladders may be an evolutionarily atrophied or reduced duct, as the closely related genera (*Halophryne* + *Allenbatrachus*) have a duct connecting the left and right swim bladder halves. Examination of the material properties of this structure would further resolve its biomechanical function.

The fact that bilateral muscle contractions in the toadfish swim bladder produce sounds with nonlinear features—such as deterministic chaos, subharmonics, and biphonation (Rice *et al.*, 2011)—raises intriguing evolutionary comparisons between the swim bladder, larynx, and songbird syrinx. While there are clear morphological and biomechanical

differences between these mechanisms, there remain a number of analogous similarities that may shed light on the evolution, convergence, and function of peripheral vocal mechanisms. One of the immediate similarities is that all three of these structures have a bilateral design, and the independent lateralized movement of tissues creates nonlinear sounds (e.g., Nowicki and Capranica, 1986; Herzel *et al.*, 1995; Larsen and Goller, 1999; Fitch *et al.*, 2002; Rice *et al.*, 2011; Elemans *et al.*, 2015). The convergent pattern of bilateral oscillating vocal structures that produce complex vocalizations and increase the vocal repertoire of vertebrates seems to be a recurring feature in the evolution of acoustic communication.

The bilateral nature of the *B. trispinosus* swim bladder as modeled here suggests a convergent system to the avian syrinx (Rice *et al.*, 2011). A number of workers have developed various models of syringeal performance (Nottebohm, 1971; Larsen and Goller, 1999; Suthers and Margoliash, 2002; Laje and Mindlin, 2005; Mindlin and Laje, 2005; Amador and Mindlin, 2008; Riede and Goller, 2010b; Elemans, 2014; Elemans *et al.*, 2015), but the biomechanical model that most closely resembles ours is that of the ring dove, *Streptopelia* sp. (Elemans *et al.*, 2008). The model of Elemans *et al.* (2008) of the ring dove syrinx shows the sides of the syrinx interacting as linearly functioning, coupled springs [Eq. (4.3) from Elemans *et al.*, 2008]. In both models, nonlinear elements of emitted sounds in each system depend on both sides vibrating, which is further corroborated by the loss of nonlinear features in toadfish calls when the nerve to one side is transected (Rice *et al.*, 2011). Additionally, both vocal organs are driven by highly specialized superfast sonic muscles (Rome *et al.*, 1996; Elemans *et al.*, 2004; Rome, 2006).

There are, however, three notable differences in the biomechanics of the toadfish and ring dove systems. The ring dove model depends on inward air flow across vibrating vocal folds and interaction across the halves of the syrinx (Elemans *et al.*, 2008), while our toadfish model depends on lateral movement and vibration of one pair of bladder muscles. Second, multiple cycles are required to produce a single sound pulse in birds, whereas the toadfish model shows that one cycle of simultaneous muscle contraction generates a sound. Last, the interaction between the lateral sides of the vocal organs is necessary for any sound generation in ring doves, but at low amplitudes, there is no interaction between sides in the toadfish model as each side is capable of producing sounds (Rice *et al.*, 2011).

Our original working hypothesis was that bilateral structures are required for nonlinear sound production—our prior study of *B. trispinosus* showed that the denervation of one bladder led to the loss of call nonlinearities (Rice *et al.*, 2011). However, there are instances in birds where unilateral structures can produce calls with complex nonlinearities (Zollinger *et al.*, 2008; Elemans *et al.*, 2014), suggesting neural instructions may be responsible for some components of nonlinear sounds in this system. In light of these contrasting findings, it may not be that bilaterally separated

structures are required to produce nonlinear vocalizations, per se, but they may substantially lower the amount of energy required to produce such sounds.

The frequency properties of sounds produced by vocal structures are determined or influenced by the vibrational frequency of associated tissues. In toadfishes, the contraction frequency of the muscle sets both the pulse repetition rate and the fundamental frequency of the sounds (Bass and Baker, 1990; Bass and Baker, 1991; Chagnaud and Bass, 2014). In songbirds, the frequency of labial vibration determines the fundamental frequency of song elements (Larsen and Goller, 1999). In the mammalian larynx, the size of the vocal folds correlates with the fundamental frequency (Herbst *et al.*, 2012).

One of the interesting differences between fish and tetrapod vocalizations is how sounds are modified once they are produced by the acoustic source. In tetrapods, the mouth, tongue, or beak can create source-filter interactions to modify the acoustic properties of the sounds (Hoese *et al.*, 2000; Laje and Mindlin, 2005; Riede and Goller, 2010b; Goller and Riede, 2013; Elemans, 2014). However, unlike toadfishes and several other groups of fishes (e.g., Bass and Baker, 1991; Chagnaud and Bass, 2014; Elemans *et al.*, 2014), and some species of frogs (Schmidt, 1992; Yamaguchi and Kelley, 2000), central motor output in general does not directly predict the acoustic properties of vocalizations in birds (Fee, 2002; Mindlin and Laje, 2005; Goller and Riede, 2013; Düring and Elemans, 2016), and it remains difficult to directly match neural output with vocal attributes (Elemans, 2014; Elemans *et al.*, 2015; but see Schmidt and Goller, 2016).

The complex biomechanical interaction between the central and peripheral vocal systems has only relatively recently attracted attention in studies of birds (Riede *et al.*, 2010; Riede and Goller, 2010b,a; Prince *et al.*, 2011; Goller and Riede, 2013), and in fishes, is still largely limited to batrachoidids (Bass and Baker, 1990; Bass and Baker, 1991; Bass *et al.*, 2000; Chagnaud *et al.*, 2011; Chagnaud *et al.*, 2012; Chagnaud and Bass, 2014). However, similarities in the basic biomechanical function of vocal organs across a wide range of vertebrates highlight the convergent mechanisms used in the production of acoustic communication signals.

SUPPLEMENTARY MATERIAL

See the supplementary material for Table S1 containing details of museum specimens analyzed.

ACKNOWLEDGMENTS

Thanks to Teresa Porri (Cornell Imaging Facility) for assistance with imaging and advice on staining, and to the Department of Ichthyology at the American Museum of Natural History for loaning toadfish specimens. S.M.H. was supported by a Hunter R. Rawlings III Cornell Presidential Research Scholarship. Other research support was provided, in part, by NSF IOS 1120925 and 1656664 to A.H.B.

Thanks to Allen Mensinger and Michael Fine for helpful feedback on the manuscript.

AUTHOR DECLARATIONS

Conflict of Interest

The authors declare no conflicts of interest.

DATA AVAILABILITY

The MATLAB codes used to run the biomechanical model, calculate isosurfaces, and generate figures and sounds are available at the following GitHub repository: <https://github.com/sm-han/toadfish>.

- Alexander, R. M. (2002). "Tendon elasticity and muscle function," *Comp. Biochem. Physiol. A*, **133**, 1001–1011.
- Alexander, R. M. (2003). "Modelling approaches in biomechanics," *Philos. Trans. R Soc. London B* **358**, 1429–1435.
- Amador, A., and Mindlin, G. B. (2008). "Beyond harmonic sounds in a simple model for birdsong production," *Chaos* **18**, 043123.
- Amorim, M. C. P., Simões, J. M., and Fonseca, P. J. (2008). "Acoustic communication in the Lusitanian toadfish, *Halobatrachus didactylus*: Evidence for an unusual large vocal repertoire," *J. Mar. Biol. Assoc. U.K.* **88**, 1069–1073.
- Barimo, J. F., and Fine, M. L. (1998). "Relationship of the swim-bladder shape to the directionality pattern of underwater sound in the oyster toadfish," *Can. J. Zool.* **76**, 134–143.
- Bass, A. H. (2023). "California singing fish," *Curr. Biol.* **33**, R208.
- Bass, A. H., and Baker, R. (1990). "Sexual dimorphisms in the vocal control-system of a teleost fish: Morphology of physiologically identified neurons," *J. Neurobiol.* **21**, 1155–1168.
- Bass, A. H., and Baker, R. (1991). "Evolution of homologous vocal control traits," *Brain Behav. Evol.* **38**, 240–254.
- Bass, A. H., Bodnar, D. A., and Marchaterre, M. A. (2000). "Midbrain acoustic circuitry in a vocalizing fish," *J. Comp. Neurol.* **419**, 505–531.
- Bass, A. H., and Chagnaud, B. P. (2012). "Shared developmental and evolutionary origins for neural basis of vocal-acoustic and pectoral-gestural signaling," *Proc. Natl. Acad. Sci. U.S.A.* **109**, 10677–10684.
- Bass, A. H., Chagnaud, B. P., and Feng, N. Y. (2015). "Comparative neurobiology of sound production in fishes," in *Sound Communication in Fishes*, edited by F. Ladich (Springer, Vienna), pp. 35–75.
- Bass, A. H., and Ladich, F. (2008). "Vocal-acoustic communication: From neurons to behavior," in *Fish Bioacoustics*, edited by A. N. Popper, R. R. Fay, and J. F. Webb (Springer, New York), pp. 253–278.
- Bass, A. H., Marchaterre, M. A., and Baker, R. (1994). "Vocal-acoustic pathways in a teleost fish," *J. Neurosci.* **14**, 4025–4039.
- Bass, A. H., and Rice, A. N. (2010). "Vocal-acoustic communication in fishes: Neuroethology," in *Encyclopedia of Animal Behavior*, edited by M. D. Breed and J. Moore (Academic Press, Oxford), pp. 558–567.
- Beckers, G. J. L., and ten Cate, C. (2006). "Nonlinear phenomena and song evolution in *Streptopelia* doves," *Acta Zool. Sin.* **52**, 482–485.
- Benko, T. P., and Perc, M. (2009). "Nonlinearities in mating sounds of American crocodiles," *Biosystems* **97**, 154–159.
- Bradbury, J. W., and Vehrencamp, S. L. (2011). *Principles of Animal Communication* (Sinauer Associates, Sunderland, MA).
- Brantley, R. K., and Bass, A. H. (1994). "Alternative male spawning tactics and acoustic signals in the plainfin midshipman fish *Porichthys notatus* Girard (Teleostei, Batrachoididae)," *Ethology* **96**, 213–232.
- Chagnaud, B. P., Baker, R., and Bass, A. H. (2011). "Vocalization frequency and duration are coded in separate hindbrain nuclei," *Nat. Commun.* **2**, 346.
- Chagnaud, B. P., and Bass, A. H. (2014). "Vocal behavior and vocal central pattern generator organization diverge among toadfishes," *Brain Behav. Evol.* **84**, 51–65.
- Chagnaud, B. P., Zee, M. C., Baker, R., and Bass, A. H. (2012). "Innovations in motoneuron synchrony drive rapid temporal modulations in vertebrate acoustic signaling," *J. Neurophysiol.* **107**, 3528–3542.

- Chiu, K.-H., Hsieh, F.-M., Chen, Y.-Y., Huang, H.-W., Shiea, J., and Mok, H.-K. (2013). "Parvalbumin characteristics in the sonic muscle of a freshwater ornamental grunting toadfish (*Allenbatrachus grunniens*)," *Fish Physiol. Biochem.* **39**, 107–119.
- dos Santos, M. E., Modesto, T., Matos, R. J., Grober, M. S., Oliviera, R. F., and Canário, A. (2000). "Sound production by the Lusitanian toadfish, *Halobatrachus didactylus*," *Bioacoustics* **10**, 309–321.
- Düring, D. N., and Elemans, C. P. H. (2016). "Embodied motor control of avian vocal production," in *Vertebrate Sound Production and Acoustic Communication*, edited by R. A. Suthers, W. T. Fitch, R. R. Fay, and A. N. Popper (Springer, New York), pp. 119–157.
- Elemans, C. P. H. (2014). "The singer and the song: The neuromechanics of avian sound production," *Curr. Opin. Neurobiol.* **28**, 172–178.
- Elemans, C. P. H., Mensinger, A. F., and Rome, L. C. (2014). "Vocal production complexity correlates with neural instructions in the oyster toadfish (*Opsanus tau*)," *J. Exp. Biol.* **217**, 1887–1893.
- Elemans, C. P. H., Rasmussen, J. H., Herbst, C. T., Düring, D. N., Zollinger, S. A., Brumm, H., Srivastava, K., Svane, N., Ding, M., Larsen, O. N., Sober, S. J., and Švec, J. G. (2015). "Universal mechanisms of sound production and control in birds and mammals," *Nat. Commun.* **6**, 8978.
- Elemans, C. P. H., Spierts, I. L. Y., Müller, U. K., van Leeuwen, J. L., and Goller, F. (2004). "Bird song: Superfast muscles control dove's trill," *Nature* **431**, 146.
- Elemans, C. P. H., Zaccarelli, R., and Herzel, H. (2008). "Biomechanics and control of vocalization in a non-songbird," *J. R. Soc. Interface* **5**, 691–703.
- Fänge, R., and Wittenberg, J. B. (1958). "The swimbladder of the toadfish (*Opsanus tau* L.)," *Biol. Bull.* **115**, 172–179.
- Fee, M. (2002). "Measurement of the linear and nonlinear mechanical properties of the oscine syrinx: Implications for function," *J. Comp. Physiol. A* **188**, 829–839.
- Fee, M. S., Shraiman, B., Pesaran, B., and Mitra, P. P. (1998). "The role of nonlinear dynamics of the syrinx in the vocalizations of a songbird," *Nature* **395**, 67–71.
- Fine, M. L. (1978). "Seasonal and geographical variation of the mating call of the oyster toadfish *Opsanus tau* L.," *Oecologia* **36**, 45–57.
- Fine, M. L. (1983). "Frequency response of the swimbladder of the oyster toadfish," *Comp. Biochem. Physiol. A* **74**, 659–663.
- Fine, M. L., King, T. L., Ali, H., Sidker, N., and Cameron, T. M. (2016). "Wall structure and material properties cause viscous damping of swimbladder sounds in the oyster toadfish *Opsanus tau*," *Proc. R. Soc. B* **283**, 20161094.
- Fine, M. L., Malloy, K. L., King, C. B., Mitchell, S. L., and Cameron, T. M. (2001). "Movement and sound generation by the toadfish swimbladder," *J. Comp. Physiol. A* **187**, 371–379.
- Fine, M. L., Malloy, K. L., King, C. B., Mitchell, S. L., and Cameron, T. M. (2002). "Sound generation by the toadfish swimbladder," *Bioacoustics* **12**, 220–222.
- Fine, M. L., and Parmentier, E. (2022). "Fish sound production: The swim bladder," *Acoust. Today* **18**, 13–21.
- Fitch, W. T., Neubauer, J., and Herzel, H. (2002). "Calls out of chaos: The adaptive significance of nonlinear phenomena in mammalian vocal production," *Anim. Behav.* **63**, 407–418.
- Forbes, J. G., Morris, H. D., and Wang, K. (2006). "Multimodal imaging of the sonic organ of *Porichthys notatus*, the singing midshipman fish," *Magn. Reson. Imaging* **24**, 321–331.
- Fouré, A., Nordez, A., and Cornu, C. (2013). "Effects of eccentric training on mechanical properties of the plantar flexor muscle-tendon complex," *J. Appl. Physiol.* **114**, 523–537.
- Fournet, M. E. H., Stabenau, E., Madhusudhana, S., and Rice, A. N. (2022). "Altered acoustic community structure indicates delayed recovery following ecosystem perturbations," *Estuar. Coast. Shelf Sci.* **274**, 107948.
- Fricke, R., Eschmeyer, W. N., and Fong, J. D. (2023). *Eschmeyer's Catalog of Fishes: Species by Family/Subfamily*, <http://researcharchive.calacademy.org/research/ichthyology/catalog/SpeciesByFamily.asp> (Last viewed June 7, 2023).
- Gignac, P. M., and Kley, N. J. (2014). "Iodine-enhanced micro-CT imaging: Methodological refinements for the study of the soft-tissue anatomy of post-embryonic vertebrates," *J. Exp. Zool. B* **322**, 166–176.
- Goller, F., and Riede, T. (2013). "Integrative physiology of fundamental frequency control in birds," *J. Physiol.* **107**, 230–242.
- Greenfield, D. W. (2001). "Toadfishes," in *FAO Species Identification Guide for Fisheries Purposes. The Living Marine Resources of the Western Central Pacific, Vol 3. Batoid Fishes, Chimaeras and Bony Fishes, Part 1 (Elopidae to Linophrynidae)*, edited by K. E. Carpenter and V. H. Niem (Food and Agricultural Organization of the United Nations, Rome, Italy), pp. 1999–2003.
- Greenfield, D. W., Winterbottom, R., and Collette, B. B. (2008). "Review of the toadfish genera (Teleostei: Batrachoididae)," *Proc. Cal. Acad. Sci.* **59**, 665–710.
- Grunst, M. L., and Grunst, A. S. (2014). "Song complexity, song rate, and variation in the adrenocortical stress response in song sparrows (*Melospiza melodia*)," *Gen. Comp. Endocrinol.* **200**, 67–76.
- Gudger, E. W. (1908). "Habits and life history of the toadfish (*Opsanus tau*)," *Bull. Bur. Fish.* **28**, 1071–1109.
- Herbst, C. T., Stoeger, A. S., Frey, R., Lohscheller, J., Titze, I. R., Gumpenberger, M., and Fitch, W. T. (2012). "How low can you go? Physical production mechanism of elephant infrasonic vocalizations," *Science* **337**, 595–599.
- Herzel, H., Berry, D., Titze, I., and Steinecke, I. (1995). "Nonlinear dynamics of the voice: Signal analysis and biomechanical modeling," *Chaos* **5**, 30–34.
- Hoese, W. J., Podos, J., Boetticher, N. C., and Nowicki, S. (2000). "Vocal tract function in birdsong production: Experimental manipulation of beak movements," *J. Exp. Biol.* **203**, 1845–1855.
- Kroodtsma, D. E. (1980). "Winter wren singing behavior: A pinnacle of song complexity," *Condor* **82**, 357–365.
- Ladich, F., and Winkler, H. (2017). "Acoustic communication in terrestrial and aquatic vertebrates," *J. Exp. Biol.* **220**, 2306–2317.
- Laje, R., and Mindlin, G. B. (2005). "Modeling source-source and source-filter acoustic interaction in birdsong," *Phys. Rev. E* **72**, 036218.
- Lancey, T. W. (1975). "Dynamics and acoustical radiation of *Porichthys notatus*' swim bladder system," *J. Morphol.* **145**, 327–335.
- Lane, E. D. (1967). "A study of Atlantic midshipman, *Porichthys porosissimus*, in the vicinity of Port Aransas, Texas," *Contrib. Mar. Sci.* **12**, 1–53.
- Larsen, O. N., and Goller, F. (1999). "Role of syringeal vibrations in bird vocalizations," *Proc. R. Soc. B* **266**, 1609–1615.
- McKibben, J. R., and Bass, A. H. (1999). "Peripheral encoding of behaviorally relevant acoustic signals in a vocal fish: Single tones," *J. Comput. Physiol* **184**, 563–576.
- McMahon, T. A. (1984). *Muscles, Reflexes, and Locomotion* (Princeton University Press, Princeton, NJ).
- Mindlin, G. B., and Laje, R. (2005). *The Physics of Birdsong* (Springer, Berlin).
- Mohr, R. A., Whitchurch, E. A., Anderson, R. D., Forlano, P. M., Fay, R. R., Ketten, D. R., Cox, T. C., and Sisneros, J. A. (2017). "Intra- and intersexual swim bladder dimorphisms in the plainfin midshipman fish (*Porichthys notatus*): Implications of swim bladder proximity to the inner ear for sound pressure detection," *J. Morphol.* **278**, 1458–1468.
- Mosharo, K. K., and Lobel, P. S. (2012). "Acoustic signals of two toadfishes from Belize: *Sanopus astrifer* and *Batrachoides gilberti* (Batrachoididae)," *Environ. Biol. Fish.* **94**, 623–638.
- Nottebohm, F. (1971). "Neural lateralization of vocal control in a passerine bird. I. Song," *J. Exp. Zool.* **177**, 229–261.
- Nowicki, S., and Capranica, R. R. (1986). "Bilateral syringeal interaction in vocal production of an oscine bird sound," *Science* **231**, 1297–1299.
- Olsson, D. M., and Nelson, L. S. (1975). "The Nelder-Mead simplex procedure for function minimization," *Technometrics* **17**, 45–51.
- Prince, B., Riede, T., and Goller, F. (2011). "Sexual dimorphism and bilateral asymmetry of syrinx and vocal tract in the European starling (*Sturnus vulgaris*)," *J. Morphol.* **272**, 1527–1536.
- Rice, A. N., and Bass, A. H. (2009). "Novel vocal repertoire and paired swimbladders of the three-spined toadfish, *Batrachomoeus trispinosus*: Insights into the diversity of the Batrachoididae," *J. Exp. Biol.* **212**, 1377–1391.
- Rice, A. N., and Bass, A. H. (2010). "Novel toadfish swimbladder morphology creates nonlinear acoustic complexities," *Integr. Compar. Biol.* **50**, e146.
- Rice, A. N., Farina, S. C., Makowski, A. J., Kaatz, I. M., Lobel, P. S., Bemis, W. E., and Bass, A. H. (2022). "Evolutionary patterns in sound production across fishes," *Ichthyol. Herpetol.* **110**, 1–12.
- Rice, A. N., Land, B. R., and Bass, A. H. (2011). "Nonlinear acoustic complexity in a fish 'two-voice' system," *Proc. R. Soc. B* **278**, 3762–3768.

- Riede, T., Fisher, J. H., and Goller, F. (2010). "Sexual dimorphism of the zebra finch syrinx indicates adaptation for high fundamental frequencies in males," *PLoS One* **5**, e11368.
- Riede, T., and Goller, F. (2010a). "Functional morphology of the sound-generating labia in the syrinx of two songbird species," *J. Anat.* **216**, 23–36.
- Riede, T., and Goller, F. (2010b). "Peripheral mechanisms for vocal production in birds—Differences and similarities to human speech and singing," *Brain Lang.* **115**, 69–80.
- Rome, L. C. (2006). "Design and function of superfast muscles: New insights into the physiology of skeletal muscle," *Ann. Rev. Physiol.* **68**, 193–221.
- Rome, L. C., Syme, D. A., Hollingworth, S., Lindstedt, S. L., and Baylor, S. M. (1996). "The whistle and the rattle: The design of sound producing muscles," *Proc. Natl. Acad. Sci. U.S.A.* **93**, 8095–8100.
- Schmidt, R. S. (1992). "Neural correlates of frog calling: Production by two semi-independent generators," *Behav. Brain Res.* **50**, 17–30.
- Schmidt, M. F., and Goller, F. (2016). "Breathtaking songs: Coordinating the neural circuits for breathing and singing," *Physiology* **31**, 442–451.
- Sisneros, J. A., and Bass, A. H. (2003). "Seasonal plasticity of peripheral auditory frequency sensitivity," *J. Neurosci.* **23**, 1049–1058.
- Sisneros, J. A., and Bass, A. H. (2005). "Ontogenetic changes in the response properties of individual, primary auditory afferents in the vocal plainfin midshipman fish *Porichthys notatus* Girard," *J. Exp. Biol.* **208**, 3121–3131.
- Skoglund, C. R. (1961). "Functional analysis of swim-bladder muscles engaged in sound production of the toadfish," *J. Biophys. Biochem. Cytol.* **10**, 187–200.
- Sprague, M. W., Fine, M. L., and Cameron, T. M. (2022). "An investigation of bubble resonance and its implications for sound production by deep-water fishes," *PLoS One* **17**, e0267338.
- Staaterman, E., Brandl, S. J., Hauer, M., Casey, J., Gallagher, A. J., and Rice, A. N. (2018). "Individual voices in a cluttered soundscape: Acoustic ecology of the Bocon toadfish, *Amphichthys cryptocentrus*," *Environ. Biol. Fish.* **101**, 979–995.
- Summers, A. P., and Koob, T. J. (2002). "The evolution of tendon—Morphology and material properties," *Comp. Biochem. Physiol. A.* **133**, 1159–1170.
- Suthers, R. A., Fitch, W. T., Fay, R. R., and Popper, A. N. (2016). *Vertebrate Sound Production and Acoustic Communication* (Springer International Publishing, Cham, Switzerland).
- Suthers, R. A., and Margoliash, D. (2002). "Motor control of birdsong," *Curr. Opin. Neurobiol.* **12**, 684–690.
- Suthers, R. A., Narins, P. M., Lin, W.-Y., Schnitzler, H.-U., Denzinger, A., Xu, C.-H., and Feng, A. S. (2006). "Voices of the dead: Complex nonlinear vocal signals from the larynx of an ultrasonic frog," *J. Exp. Biol.* **209**, 4984–4993.
- Tokuda, I., Riede, T., Neubauer, J., Owren, M. J., and Herzog, H. (2002). "Nonlinear analysis of irregular animal vocalizations," *J. Acoust. Soc. Am.* **111**, 2908–2919.
- Tower, R. W. (1908). "The production of sound in the drumfishes, the sea-robin and the toadfish," *Ann. N.Y. Acad. Sci.* **28**, 149–180.
- Vaz, D. F. B. (2020). "Morphology and systematics of batrachoidiformes (Percormorphacea: Teleostei)," Ph.D. thesis, The College of William and Mary, Williamsburg, VA.
- Vaz, D. F. B., and Hilton, E. J. (2020). "The caudal skeleton of Batrachoidiformes (Teleostei: Percormorphacea): A study of morphological diversity, intraspecific variation, and phylogenetic inferences," *Zool. J. Linn. Soc.* **189**, 228–286.
- Wilden, I., Herzog, H., Peters, G., and Tembrock, G. (1998). "Subharmonics, biphonation, and deterministic chaos in mammal vocalization," *Bioacoustics* **9**, 171–196.
- Yamaguchi, A., and Kelley, D. B. (2000). "Generating sexually differentiated vocal patterns: Laryngeal nerve and EMG recordings from vocalizing male and female African clawed frogs (*Xenopus laevis*)," *J. Neurosci.* **20**, 1559–1567.
- Zollinger, S. A., Riede, T., and Suthers, R. A. (2008). "Two-voice complexity from a single side of the syrinx in northern mockingbird *Mimus polyglottos* vocalizations," *J. Exp. Biol.* **211**, 1978–1991.